Korean J. Chem. Eng., **30**(2), 501-507 (2013)
DOI: 10.1007/s11814-012-0170-5

A model for estimating agglomerate sizes of non-magnetic nanoparticles in magnetic fluidized beds

Li Zhou*,, Feng Zhang*, Tao Zhou*,†, Hiroyuki Kage***, and Yoshihide Mawatari*****

*Key Laboratory of Resources Chemistry of Nonferrous Metals, Central South University, Changsha 410083, Hunan, China
**Department of Mechanical Engineering, Hunan Institute of Technology, Hengyang 421002, Hunan, China
***Department of Applied Chemistry, Kyushu Institute of Technology, 1-1 Sensui-cho, Tobata, Kitakyushu 804-8550, Japan
(*Received 27 June 2012 • accepted 2 October 2012*)

Abstract−The behavior of SiO_2, TiO_2 and ZnO non-magnetic nanoparticles and the effects of processing parameters on agglomerate sizes were investigated systematically in a magnetic fluidized bed (MFB) by adding coarse magnets. A mathematical model is developed based on energy balance among the agglomerate collision energy, magnetic energy, energy generated by turbulent shear and cohesive energy to predict the agglomerate sizes. The results showed that slugging of the bed disappeared and the measured agglomerate sizes decreased, so that the fluidization quality of non-magnetic nanoparticles was significantly improved by adding coarse magnets due to introduction of magnetic field. The average agglomerate sizes predicted by this model are in agreement with the experimental data.

Key words: Non-magnetic Nanoparticles, Magnetic Fluidized Bed, Agglomerate Size, Energy Balance Model, Coarse Magnets

INTRODUCTION

Nanoparticles have received much attention due to their increasing potential for extensive industrial applications, such as advanced materials, food, pharmaceuticals, and nanosize catalysts, etc. However, strong interparticle forces always result in undesired large agglomerates, handling trouble and lower productivity. It is proved that magnetic fluidization is an effective method to improve fluidization quality of nanoparticles [1-3]. Previous studies [4,5] showed that the fluidization quality of microsized particles was significantly improved due to addition of magnetic field. However, the absence of study about agglomerate sizes seriously affects its industrial scale application.

Agglomerate sizes and the agglomerate size distribution in gas-solid fluidized beds of nanoparticles are the most important factors influencing the fluidization quality of nanoparticles and can be measured by using the experimental methods, such as freezing-agglomerate method [6], high-speed digital charge-coupled device (CCD) camera [7], laser-based planar imaging analysis [8], etc. The measurement and prediction of agglomerate sizes based on a model of force balance in a conventional fluidized bed of cohesive particles (micron size) were reported and discussed by several researchers [9-12]. Xu and Zhu [13] proposed a model to predict agglomerate sizes of cohesive particles (micron size) on the basis of the energy balance among the agglomerate collision energy, the cohesive energy and the energy generated by vibration. Matsuda et al. [14] developed a comprehensive model based on the energy balance model with respect to energy consumption for disintegration of agglomerates to predict agglomerate sizes of cohesive particles (micron size) in a vibro-fluidized bed. Guo et al. [15] calculated the agglomerate sizes of the SiO_2 nanoparticles in the acoustic fluidized bed by assuming the combination of collision energy and adhesive energy is equal to sound energy. Wang et al. [16] estimated the agglomerate sizes of nanoparticles in the vibro-fluidized bed based on the combination of Richardson-Zaki scaling law and Stokes law. Some studies [17,18] used numerical simulations to investigate fluidization behaviors of ferromagnetic particles in a magnetically fluidized bed (MFB) based on two fluid model and kinetic theory of granular flow. In these works, some focused on prediction of agglomerate sizes of micron size particles [7,11-13], and another is for forced field, such as vibration filed [13,14,16] or sound field [15]. However, the work of estimating agglomerate sizes of non-magnetic nanoparticles prepared by liquid phase method in MFB by using energy balance model has not been reported so far.

In this study, an experimental study is conducted to determine the effects of processing parameters on agglomerate sizes of SiO_2, TiO_2 and ZnO non-magnetic nanoparticles prepared by liquid phase method in MFB. A model is developed based on energy balance among the agglomerate collision energy, magnetic energy, energy generated by turbulent shear and cohesive energy to predict the agglomerate sizes of non-magnetic nanoparticles.

EXPERIMENTAL SETUP

A schematic diagram of the MFB is shown in Fig. 1. The cylindrical transparent column of organic glass with 50 mm inner diameter and 1,200 mm height was used in the experiments. Sintered porous distributor was used to introduce compressed air, preliminary dried by a silica gel column, into the fluidization chamber. The superficial gas velocity and pressure drop were measured by a rotameter and U-type manometer, respectively. The fluidized agglomerates were taken out from the different axial and radial locations of a bed (see Fig. 1) with a self-made sampling ladle and examined

†To whom correspondence should be addressed.
E-mail: zhoutao@csu.edu.cn

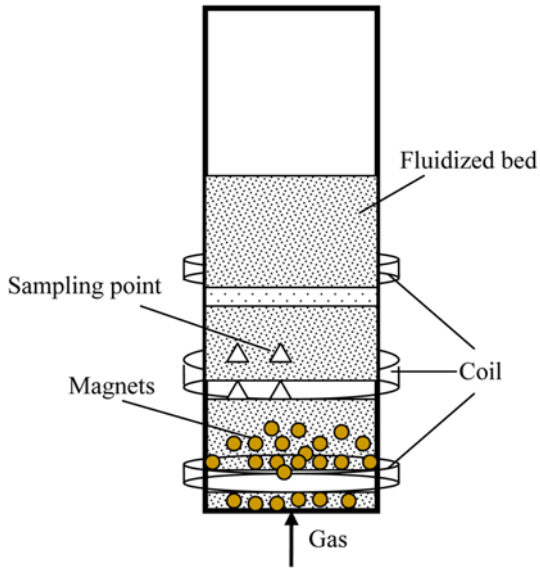

Fig. 1. Schematic diagram of experimental set-up.

Table 1. Properties of nanoparticles and coarse magnets

Nanoparticles	Primary particle size (nm)	Bulk density (kg/m^3)	Particle density (kg/m^3)
SiO_2	10	86.6	2560
TiO_2	30	261	3850
ZnO	16	341	5600
Coarse magnets	2 mm Steel spheres with density of 7,780 kg/m^3		

by positive position metallographic microscope. The properties of non-magnetic nanoparticles and coarse magnets used in experiments are summarized in Table 1.

Homogeneous axially magnetic field was generated by a 300 laps solenoid (80 mm inner diameter, 200 mm outer diameter and height of 35 mm) energized by a DC electric supply with a current (I) within the range from 0 to 10 A. The magnetic field intensity (kA/m) was calculated from $H=\sum_{i=1}^{4}\frac{N*R^2*I}{2*(R^2+x_i^2)^{3/2}}$ with x_i=0, 0.1 m, 0.2 m and 0.3 m.

Where N=300 and R is solenoid geometric radius, defined as: $R=\sqrt{R_1R_2}$

MODEL ANALYSIS ON AGGLOMERATES IN MFB

In the MFB, the following simplified assumptions are made in order to set up the model of energy balance: (a) agglomerates can be represented as spheres with the same properties; (b) the size of agglomerates is represented by a mean diameter of d_a; (c) the wall effect and elutriation are not considered; (d) the effect of electrostatic forces and liquid bridging forces is not considered as the air is dried by a silica gel column. In a magnetic fluidized bed of non-magnetic nanoparticles, the energy acting on agglomerate include energy generated by turbulent shear E_{tur}, collision energy E_{col}, cohesive energy E_{coh} and magnetic energy E_{mag}. Accordingly, the following energy balance may be obtained at the breaking critical point for the fluidized agglomerates.

$$E_{col}+E_{mag}+E_{tur}=E_{coh} \quad (1)$$

1. Collision Energy, E_{col}

The collision agglomerates behave to accelerating or decelerating motion, and E_{col} is obtained as the following:

$$E_{col}=\int_0^{\alpha_{max}}F_{col}d\alpha \quad (2)$$

Based on the model of Zhou and Li [7], the agglomerates are assumed as elastic bodies, and the relative collision velocity between two agglomerates is V.

$$\alpha_{max}=(0.313V^2\pi^3k\rho_a)^{2/5}d_a \quad (3)$$

The collision force between two agglomerates is expressed by

$$F_{col}=n\alpha^{3/2} \quad (4)$$

Substituting the expression Eq. (3) and (4) into Eq. (2) gives

$$E_{col}=\frac{1}{24}\pi\rho_a d_a^3V^2 \quad (5)$$

Based on the correlation of Iwadate and Horio [11], the relative velocity V between the two agglomerates in collision can be estimated as

$$V=(1.5\overline{P}_{n,s}D_bg\varepsilon_b)^{1/2} \quad (6)$$

where $\overline{P}_{s,n}\approx0.077$ is the dimensionless average particle pressure of nonsticky system; ε_b is the bed voidage, $\varepsilon_b\approx0.5$; D_b is the bubble diameter in MFB and is given by [19]

$$D_b=0.652[A_t(u_g-u_{mf})]^{2/5} \quad (7)$$

Where A_t is the cross-section area of the bed; the minimum fluidization velocity u_{mf} of agglomerates was from experimental data.

2. Magnetic Energy, E_{mag}

Previous studies showed that fluidization quality was improved significantly due to introduction of magnetic field energy. It was found that the introduction of the magnetic field energy could bring two main effects in the experiments. First, the magnetic field lines could break bubbles; and the second, the movement of adding coarse magnets in MFB could break up the agglomerates. However, the magnetic forces or energy in the magnetic field not directly act on the non-magnetic nanoparticles. Therefore, the effective magnetic energy is defined in order to characterize the acting energy of non-magnetic nanoparticle agglomerates due to introduction of magnetic field.

The comprehensive analysis on the experimental studies shows that the parameters of influencing the effective magnetic energy are as follows: magnetic field strength, H, amount of coarse magnets, x, density of agglomerates, ρ_a, diameter of agglomerates, d_a, relative velocity of agglomerate collision, V, and magnetic permeability of the vacuum, μ_0. Therefore, the general variable function can be written as follows:

$$E_{mag}=F(H, x, \rho_a, d_a, V, \mu_0) \quad (8)$$

The above relationship can be expressed using the power function,

$$E_{mag}^2=K*\mu_0^p*x^t*H^j*\rho_a^e*d_a^f*V^q \quad (9)$$

According to the principle of dimensional consistency, it can be ob-

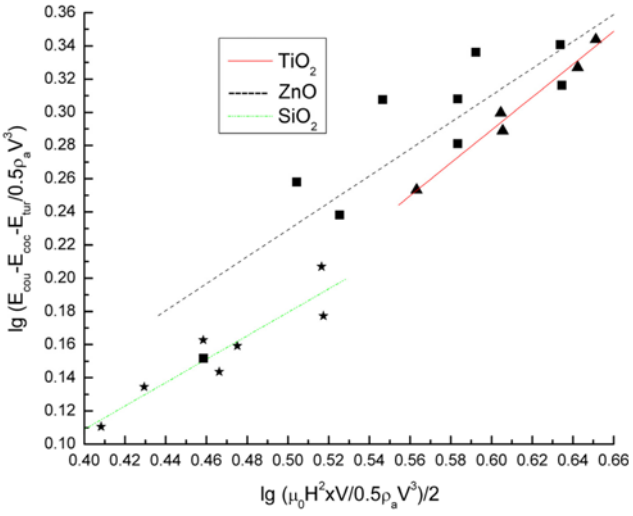

Fig. 2. Linear fitting curves of values of s and K‴.

Table 2. Values of s and K‴ for SiO_2, TiO_2 and ZnO nanoparticles

Nanoparticles	s	K‴
SiO_2	0.8331	0.5846
TiO_2	1.0722	0.4414
ZnO	0.9436	0.5570

tained

$$E_{mag}=K'''(\mu_0 H^2 xV)^{\frac{s}{2}}*(0.5\rho_a V^3)^{\frac{2-s}{2}} \quad (9)$$

According to Eq. (1),

$$E_{coh}-E_{col}-E_{tur}=K'''(\mu_0 H^2 xV)^{\frac{s}{2}}*(0.5\rho_a V^3)^{\frac{2-s}{2}} \quad (10)$$

The values of s and K‴ of SiO_2, TiO_2 and ZnO nanoparticles can be obtained based on linear fitting through the experimental data based on Eq. (10) (see Fig. 2), as shown in Table 2.

3. Cohesive Energy, E_{coh}

In the gas-solid fluidization state, nanoparticles trend to agglomerate due to the action of the interparticle attractive force (van der Waals force). To break up agglomerates, the tensile strength due to cohesive forces within the agglomerates must be overcome, and the energy required for this process has to be equal to or larger than the cohesion energy, E_{coh}. Therefore, the cohesion energy is defined as

$$E_{coh}=\int_{Z_0}^{Z}\frac{\pi}{4}d_a^2\sigma_t d\delta \quad (11)$$

where σ_t is the tensile strength of the agglomerate; δ is the displacement of the two parts of the agglomerate at the breakage or the distance between the two departing particles; Z_0 is the initial distance between the two adjacent particles and Z is the maximum distance which the tensile strength of the agglomerate remains in effect.

According to theories of Molerus [20] and Rumpf [21], inter-agglomerate force transmitted through the particles collision, and the tensile strength of the agglomerate can be calculated as

$$\sigma_t=\frac{1-\varepsilon_a}{\varepsilon_a}\cdot\frac{F_c}{d_p^2} \quad (12)$$

where ε_a is the agglomerate voidage and F_c is the adhesion forces at a single contact point.

According to the Israelachvili's theory [22] of the intermolecular and surface forces or Derjaguin [23] approximation, van der Waals force is given by

$$F_{van}=\frac{Ad_p}{24\delta^2} \quad (13)$$

where d_p is the primary particle size diameter of the particles. A is the Hamaker constant.

It can be found from the experiments that van der Waals force dominates over other types of interparticle force. Considering the number of contact points per particle, the actual adhesion forces F_c is as follows: [24,25]

$$F_c=1.61\frac{Ad_p}{24\delta^2} \quad (14)$$

Substituting Eq. (12) and Eq. (14) into Eq. (11), cohesion energy can be presented as

$$E_{coh}=\int_{z_0}^{z}\frac{\pi}{4}d_a^2\frac{Ad_p}{24\delta^2}1.61\frac{1-\varepsilon_a}{\varepsilon_a}\frac{1}{d_p^2}d\delta=\frac{\pi}{96}d_a^2 1.61\frac{1-\varepsilon_a}{\varepsilon_a}\frac{A}{d_p}\left(\frac{1}{Z_0}-\frac{1}{Z}\right) \quad (15)$$

As Z is much higher than Z_0, cohesion energy can simplified as

$$E_{coh}=\frac{\pi}{96}d_a^2 1.61\frac{1-\varepsilon_a}{\varepsilon_a}\frac{A}{d_p}\frac{1}{Z_0} \quad (16)$$

According to the hypothesis of Zhou and Li [7], ε_a can be given as

$$\varepsilon_a=1-\frac{\rho_a}{\rho_p} \quad (17)$$

where ρ_p is primary density and the agglomerate density ρ_a of cohesive particles is 1.15 times the bulk density for agglomerates bound loosely. It is known by calculation that the agglomerate voidage of SiO_2, TiO_2 and ZnO nanoparticles is 0.961, 0.922 and 0.930, respectively.

The distance between particles or agglomerates, δ, is 1.5-4.0×10^{-10} m and we choose $\delta=4.0\times10^{-10}$ m. Citing from the physical properties handbook, the dielectric constant, index of refraction and Hamaker constant of nanoparticles are shown in Table 3.

4. Energy Generated by Turbulent Shear, E_{tur}

According to two-phase flow model, the velocity of agglomerates is closed to the minimum fluidization velocity in the emulsion phase. At the minimum fluidization velocity, the kinetic or drag force for particles or agglomerates in a fluidized bed in turbulent flow is given by [26]:

$$F_{drag}=0.055\pi\rho_f d_a^2 u_g^2 \varepsilon^{-4.8} \quad (18)$$

Energy generated by hydrodynamics shear is obtained as

Table 3. The dielectric constant, index of refraction and Hamaker constant of nanoparticles

Nanoparticles	ε_1	N_1	$A\times10^{-20}$ (J)
SiO_2	3.7	1.5442	8.221
TiO_2	40-60	2.493	39.73
ZnO	8.656	1.9	21.42

$$E_{drag}=2\int_{0}^{Z_0+\alpha}F_{drag}d\delta \quad (19)$$

Substituting Eq. (18) into Eq. (19) gives

$$E_{drag}=0.11\pi\rho_f d_a^2 u_g^2 \varepsilon^{-4.8}(\alpha+Z_0) \quad (20)$$

$$\alpha=\left(\frac{5}{16}V^2\pi^2 k\rho_a\right)^{2/5}d_a \quad (21)$$

where k is a function of Poisson's ratio and Young's modulus E, k is assumed as 3.0×10^{-6} Pa^{-1} [27] in this model.

Substituting Eqs. (5), (9), (16) and (20) into Eq. (1), the energy balance model as the following:

$$\frac{\pi}{96}d_a^2 1.61\frac{1-\varepsilon_a}{\varepsilon_a}\frac{A}{d_p}\frac{1}{Z_0}=\frac{1}{24}\pi\rho_a d_a^3 V^2+K'''(\mu_0 H^2 xV)^{\frac{s}{2}}*(0.5\rho_a V^3)^{\frac{2-s}{2}}$$
$$+0.11\pi\rho_f d_a^2 u_g^2\varepsilon^{-4.8}(\alpha+Z_0) \quad (22)$$

The various parameters are substituted into Eq. (22), and the agglomerate size can be calculated with the difference method.

RESULTS AND DISCUSSION

1. Agglomerate Sizes in a Conventional Fluidization Bed

The experiment results show that SiO_2, TiO_2 and ZnO nanoparticles are difficult to be fluidized in a conventional fluidization bed, and there exist three stages: slugging, channeling and partial agglomerates fluidization. Visual observation reveals that the top-bed of SiO_2 and TiO_2 nanoparticles gradually fluidized with increasing gas velocity, albeit the larger agglomerates rest the bottom of the fixed bed with maximum size around 2 mm. Differing from the two above-mentioned nanoparticles, ZnO nanoparticles are in formation of smaller agglomerates.

In conventional fluidization bed, according to the experimental observations, the three nanoparticle agglomerates sizes at the top-bed showed a broad size distribution at 0.1132 m/s. This wide distribution was suggested as an indication of the existence of different stages of aggregation. SiO_2 and TiO_2 agglomerates were larger than ZnO agglomerates with exhibiting a wide distribution. The average agglomerate size of SiO_2 nanoparticles is 199.5 μm at the top-bed and 264.5 μm at middle-bed, respectively. For TiO_2 nano-particles, average agglomerate size is 170 μm and 245 μm at middle-bed, respectively. For ZnO nanoparticles, average agglomerate size is 102 μm at the top-bed and 158 μm at middle-bed, respectively.

2. Agglomerate Sizes in Magnetic Fluidized Beds

Figs. 3-5 illustrate the variations in average agglomerate sizes with processing parameters for SiO_2, TiO_2 and ZnO nanoparticles by adding coarse magnets. The experimental results showed that the agglomerate sizes of SiO_2 and ZnO nanoparticles decreased with increasing magnetic field intensity (see Figs. 3-4). However, it was found that coarse magnets would condense at high magnetic field intensity.

Measured agglomerate sizes of ZnO nanoparticles also decrease with increasing the magnetic field intensity. When magnetic field intensity is 8.36-11.14 kA/m, agglomerate sizes are significantly decreased. With increasing further the magnetic field intensity, decreasing variety of ZnO nanoparticle agglomerate sizes tends to slow down. This is because the bed has defluidization, and is a fixed-bed in the bottom of the bed. With increasing magnetic field intensity, the fluidization region increase. The agglomerates in the fixed-bed stream to the dilute phase region of fluidized bed top, and the agglomerate sizes decrease. The bed begins to fluidize at the magnetic field intensity of 16.71 kA/m. At the same time, coarse magnets also begin condensing.

With increasing the magnetic field intensity, TiO_2 nanoparticle

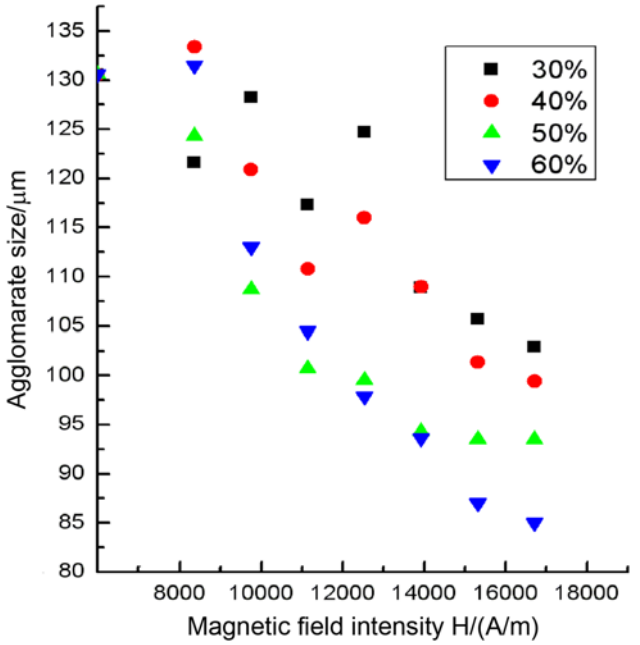

Fig. 3. Effect of magnetic field intensity on the top-bed agglomerates size of ZnO nanoparticles at different amount of coarse magnets and superficial gas velocity of 0.1132 m/s.

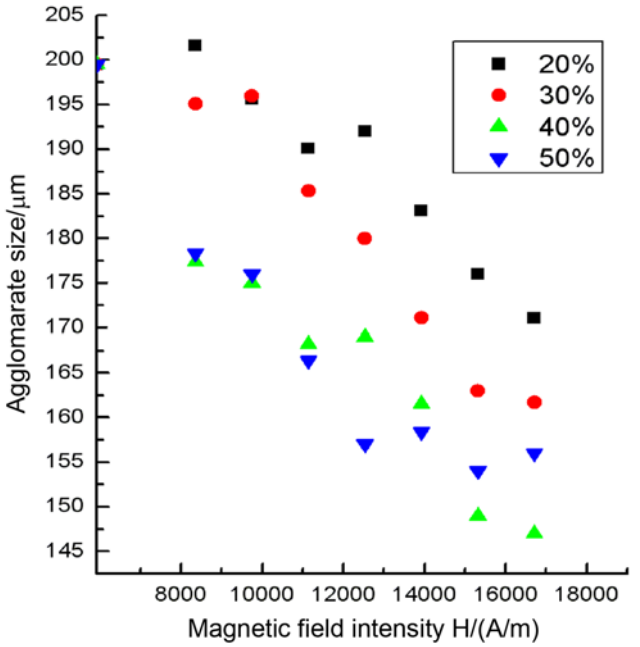

Fig. 4. Effect of magnetic field intensity on the top-bed agglomerates size of SiO_2 nanoparticles at different amount of coarse magnets and superficial gas velocity of 0.1132 m/s.

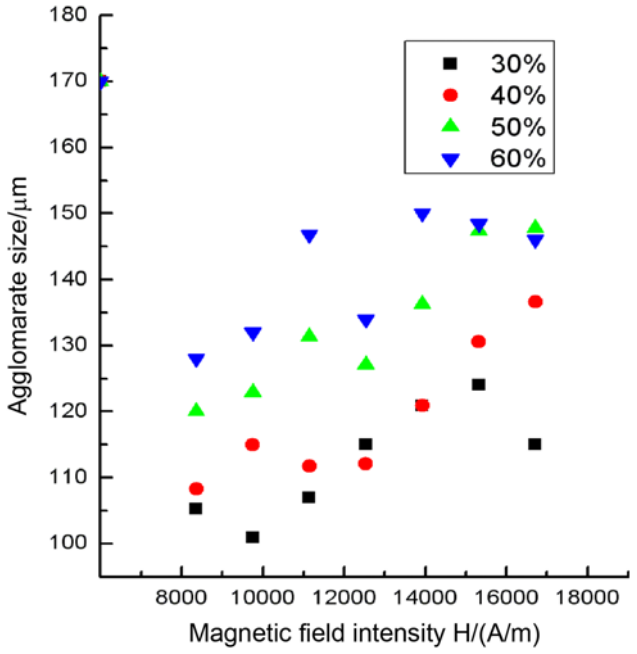

Fig. 5. Effect of magnetic field intensity on the top-bed agglomerates size of TiO_2 nanoparticles at different amount of coarse magnets and superficial gas velocity of 0.1132 m/s.

agglomerate sizes showed a trend of first increase and then stabilized or slightly decreased (see Fig. 5). This is because when fluidized beds have defluidization, a fixed-bed of large agglomerates is formed in the bed bottom. With the increase in the magnetic field intensity, part of large agglomerates begins to fluidize. Increasing the amount of coarse magnets (the steel spheres) to 50% (wt) at the magnetic field intensity of 13.93 kA/m, particle beds begin to fluidize. At the same time, coarse magnets also happen condensing so that agglomerate size became stable.

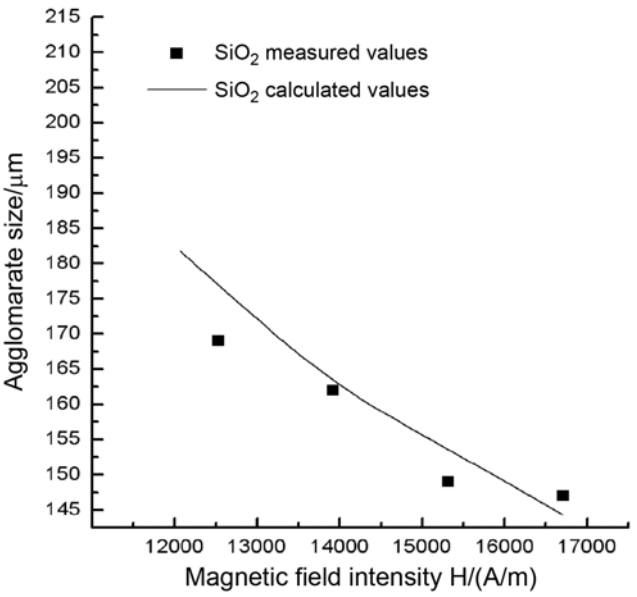

Fig. 6. Experimental and model predicted values with 40% (wt) of coarse magnets and a superficial gas velocity of 0.1132 m/s.

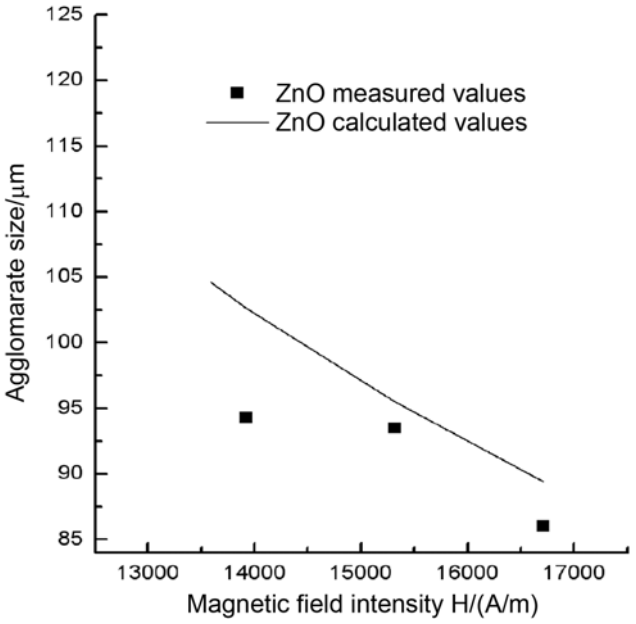

Fig. 7. Experimental and model predicted values with 50% (wt) of coarse magnets and a superficial gas velocity of 0.1132 m/s.

3. Estimation of Agglomerate Sizes

Substituting various parameters into Eq. (22), the estimated agglomerate sizes can be obtained. Figs. 6-8 show examples of the comparison of measured and estimated agglomerate sizes for SiO_2, ZnO and TiO_2 non-magnetic nanoparticles (all non-magnetic nanoparticle agglomerates were fluidized) at the superficial gas velocity of 0.1132 m/s. It can be seen from Fig. 6 that the agglomerate sizes of SiO_2 nanoparticles calculated by this model are in reasonable agreement with the experimental values when magnetic field inten-

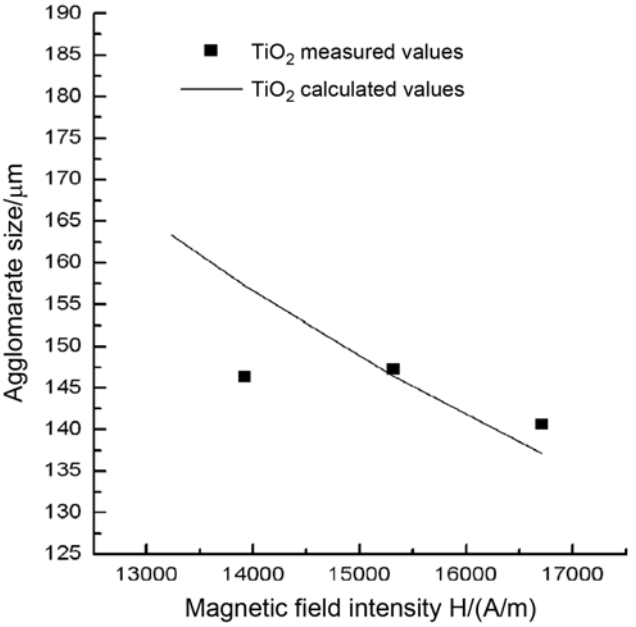

Fig. 8. Experimental and model predicted values with 40% (wt) of coarse magnets and a superficial gas velocity of 0.1132 m/s.

sity is in the range of 13-17 kA/m and the adding amount of 40% (wt) coarse magnets. For ZnO nanoparticles, the agglomerate sizes calculated by this model are in agreement with the experimental values only when magnetic field intensity is in the range of 15-16 kA/m and the adding amount of 50% (wt) coarse magnets (see Fig. 7). This is because nanoparticles have different optimal operating conditions due to different physical and chemical properties. For TiO_2 nanoparticles, the agglomerate sizes calculated by this model are in agreement with the experimental values when magnetic field intensity is in the range of 15-16.5 kA/m and the adding amount of 40% (wt) coarse magnets (see Fig. 8). It can be concluded that non-magnetic nanoparticles can be fluidized in the form of smaller agglomerates if the suitable operating conditions, including magnetic field intensity, adding amount of coarse magnets and superficial gas velocity, etc. are chosen.

CONCLUSION

A mathematical model to predict agglomerate sizes in MFB of non-magnetic nanoparticles was developed based on the balance of the agglomerate collision energy, magnetic field energy, energy generated by hydrodynamics shear and cohesive energy. The agglomerate sizes of non-magnetic nanoparticles can be estimated by this model. The agglomerate sizes calculated by this model are in reasonable agreement with the experimental values at the suitable operating conditions. Experimental and model analysis showed that the agglomerating fluidization quality of non-magnetic nanoparticles can be improved significantly with increasing magnetic intensity and adding amount of the coarse magnets.

ACKNOWLEDGEMENTS

The authors acknowledge with gratitude the financial support of the National Natural Science Foundation of China (No. 20776163) and the Research Fund for the Doctoral program of Higher Education from the Ministry of Education of China (No. 20070533121) and the NSFC-JSPS cooperation program.

NOMENCLATURE

A : hamaker constant [J]
A_t : cross-section area of the fluidized bed [m^2]
B : boltzmann constant (=1.381×10^{-23} J/K)
d_a : diameter of agglomerate [μm]
d_{ac} : the calculated diameter of agglomerate [μm]
d_{am} : the measured diameter of agglomerate [μm]
d_{ai} : diameter of agglomerate i, (i=1, 2) [μm]
d_p : diameter of primary particles [μm]
D_b : diameter of bubbles in the fluidized bed [m]
E : Young's modulus [Pa]
E_{coh} : cohesion energy of agglomerates [J]
E_{col} : collision energy between agglomerates [J]
E_{tur} : energy generated by turbulent shear [J]
E_{mag} : magnetic energy [J]
F_c : the interparticle forces at single contact point [N]
F_{col} : collision force between agglomerates [N]
F_{van} : the van der Waals force [N]
h : Planck's constant (=6.626×10^{-34} J•s)
H : magnetic field strength [kA/m]
I : current [A]
k : function of Poisson's ratio and Young's modulus [Pa^{-1}]
m_i : mass of agglomerate i, (i=1, 2) [kg]
N_i : index of refraction of particle (i=0, 1)
N : solenoid laps
$\overline{P}_{s,n}$: dimensionless average particle pressure
R : solenoid geometric radius [m]
R_1 : solenoid inner diameter [m]
R_2 : solenoid outer diameter [m]
u_g : superficial gas velocity [m/s]
u_{mf} : minimum fluidization velocity [m/s]
x : the amount of coarse magnets [%]
V : relative velocity of agglomerate [m/s]
Z_0 : initial distance between two agglomerates [m]
Z : displacement within which the tensile strength of the agglomerate remains in effect [m]

Greek Letters

α : compression displacement [m]
α_{max} : maximum compression displacement [m]
δ : the displacement of the two parts of the agglomerate at the breakage [m]
ε_a : agglomerate at the breakage [m]
ε_b : average bed voidage, dimensionless
μ_f : gas viscosity [Pa·S]
μ_0 : magnetic permeability of the vacuum
υ : Poisson's ratio
υ_e : main electronic absorption frequency in the UV region
ρ_a : density of agglomerate [kg/m^3]
ρ_b : bulk density of bed [kg/m^3]
ρ_p : density of primary particle [kg/m^3]
σ : tensile strength of the agglomerate [Pa]
σ_{max} : maximum tensile strength of the agglomerate [Pa]

REFERENCES

1. J. A. Quevedo, J. Flesch, R. Pfeffer and R. N. Dave, *Chem. Eng. Sci.*, **62**, 2608 (2007).
2. P. Zeng, T. Zhou and J. S. Yang, *Chem. Eng. Process.*, **47**, 101 (2008).
3. Q. Yu, R. N. Dave, C. Zhu, J. A. Quevedo and R. Pfeffer, *AIChE J.*, **51**, 1971 (2005).
4. Q. S. Zhu and H. Z. Li, *Powder Technol.*, **86**, 179 (1996).
5. X. S. Lu and H. Z. Li, *Powder Technol.*, **107**, 66 (2000).
6. A. W. Pacek and A. W. Nienow, *Powder Technol.*, **60**, 145 (1990).
7. T. Zhou and H. Z. Li, *Powder Technol.*, **101**, 57 (1999).
8. X. S. Wang, V. Palero, J. Soria and M. J. Rhodes, *Chem. Eng. Sci.*, **61**, 5476 (2006).
9. S. Morooka, K. Kusakabe, A. Kobata and Y. Kato, *J. Chem. Eng. Japan*, **21**, 41 (1988).
10. M. Horio and Y. Iwadate, Proc. of the 5th World Congress of Chem. Eng., 2nd Int. Particle Technol. Forum, 571 (1996).
11. Y. Iwadate and M. Horio, *Powder Technol.*, **100**, 223 (1998).
12. T. Zhou, H. Z. Li and S. Kunio, *Adv. Powder Technol.*, **17**, 159 (2006).
13. C. B. Xu and J. Zhu, *Chem. Eng. Sci.*, **60**, 6529 (2005).

14. S. Matsuda, H. Hatano, T. Muramoto and A. Tsutsumi, *AIChE J.*, **50**, 2763 (2004).
15. Q. J. Guo, X. P. Yang, W. Z. Shen and H. E. Liu, *Chem. Eng. Process.*, **46**, 307 (2007).
16. H. Wang, T. Zhou, J. S. Yang, J. J. Wang, H. Kage and Y. Mawatari, *Chem. Eng. Technol.*, **33**, 388 (2010).
17. Y. H. Wang, K. T. Gui, M. H. Shi and C. F. Li, *J. Jiangsu Univ.* (Natural Science Edition), **29**, 419 (2008).
18. X. Li, D. Sun, J. H. Chen, S. Wang, Y. H. Bai and H. L. Lu, Chem. Eng. Chinese Univ., **24**, 52 (2010).
19. S. Mori and C. Y. Wen, *AIChE J.*, **21**, 109 (1975).
20. O. Molerus, *Powder Technol.*, **33**, 81 (1982).
21. H. Rumpf, *Chem. - Ink. -Tech.*, **42**, 538 (1970).
22. J. N. Israelachvili, Academicx Press, Orlando, FL, London, 88 (1985).
23. B. V. Derjaguin, *Kolloid Zeits*, **69**, 155 (1934).
24. E. Jaraiz, S. Kiruma and O. Levenspiel, *Powder Technol.*, **72**, 23 (1992).
25. H. Krupp, *Adv. Colloid Interface Sci.*, **1**, 111 (1967).
26. A. R. Khan and J. F. Richardson, *Chem. Eng. Sci.*, **45**, 255 (1990).
27. S. P. Timoshenko and J. N. Goodier, McGraw-Hill, New York, 68 (1970).